Temporal Imaging for accurate time, space and energy localization of Photoelectric events in monolithic scintillators

Alain Iltis[a], Hichem Snoussi[b], Luc Rodrigues de Magalhaes[a] and Ghislain Zeufack Tadonkeng[a]
[a] Damavan Imaging, 1 rue Gustave Eiffel, 10430 Rosieres Pres Troyes France
[b] University of Technology of Troyes, UMR CNRS 6281, 12, rue Marie Curie, 10010 Troyes, France
Email: alain.iltis@damavan-imaging.com, snoussi@utt.fr

ABSTRACT

In this communication, we propose an original temporal imaging concept for accurate spatio-temporal localization of scintillation events within a monolithic scintillator and a digital Si-PM matrix. Jointly analyzing the light distribution and the arrival time distribution of the first detected photons, it was possible to better recognize a photoelectric event and to accurately localize it in space, time and energy.

Keywords: Gamma ray detection, monolithic scintillation, digital SiPM, temporal imaging

1. INTRODUCTION

In the Anger γ camera concept,[5] the absorption of the γ ray creates a scintillation event. The γ ray direction of incidence is controlled through absorption on a lead collimator. The UV scintillation light is emitted isotropically. The light is then channelled through the plane by reflection on the interfaces.The number of photons detected on the scintillation plane decreases roughly as $1/R$. This property is used to find the center of the distribution of photons and thus gives the X,Y coordinates of the scintillation event. However, many drawbacks limit the efficacy of such system: noisy images, undesired edge effects (need for bigger crystals), low resolution.[8] NaI(Tl) Gamma cameras have been used in the past for PET,[9].[12] However, the localization of the events was too coarse. In addition, the stopping power of NaI(Tl) was too low and Compton effect was an issue.

The use of monolithic scintillators such as the LaBr3:Ce is a promising detector concept for application in time of flight (TOF) positron electron tomography (PET). Monolithic scintillators[2] exhibit a number of interesting properties such as excellent energy resolution, high γ photon capture efficiency and relatively simple detector assembly. Monolithic scintillators should be also cheaper to produce than arrays of pixels. This detector concept is all the more interesting with the availability of Si-PMT which offer high gain, fast response, insensitivity to magnetic fields and potential cost effectiveness.

In this work, we consider a monolithic scintillator crystal of thickness 20 mm. The lower surface is polished with a layer of segmented Si-PMT glued to the crystal. Once a photoelectric event $E(X, Y, Z, T)$ takes place inside the crystal at position (X, Y, Z) and time T, the scintillation light is emitted isotropically following the scintillator emission light curve. Figure 1 illustrates the behavior of emitted photons after the scintillation event: (a) photons emitted inside the cone are detected by the photodetector, (b) photons emitted outside the cone in the downside direction are reflected before being scattered by the upper plane of the crystal, and (c) photons emitted in the upper direction will be scattered in a random direction. All photons emitted outside the cone will be subject to at least one scattering and thus have a longer light path in the crystal and thus will impact later the photo-detectors. Between the crystal and the detector, an optical interface is used. Thus, there is a critical angle θ_c above which the photon will be reflected. The un-scattered photons will thus be located in a cone whose summit is the event position and whose opening angle is θ_c. If n_c is the crystal index and n_g is the index of the glue between the crystal and the Si-PMT, the critical angle is $\theta_c = arcsin(n_g/n_c)$.

Hence, the image of the un-scattered photons on the detector plane will be a disc $\mathcal{D}$ centered on the location of the interaction (X, Y) and whose diameter will be $(L - Z) * tan(\theta_c)$. On a pixellized SiPM detector, at least two distributions could be obtained: (i) the light distribution which contains the number of detected photons

Further author information: (Send correspondence to Alain Iltis)
Alain Iltis.: E-mail: alain.iltis@damavan-imaging.com,
Hichem Snoussi: E-mail: snoussi@utt.fr

by pixel (photon counting) and (ii) the time distribution of the first detected photons. Combining the light distribution and the first arrival time distribution will allow :

- To find the center and the diameter of the disc of un-scattered photons. In fact, the critical disc $\mathcal{D}$ is quickly filled by the un-scattered photons. The scattered photons may be later detected outside $\mathcal{D}$, which remains, however, highly dense compared to the whole detection plane. This will allow to spatially localize the scintillation event (X, Y and Z).
- More interestingly, by putting a high statistical weight on the first photons, a ray tracing allows to better constrain X, Y and to accurately timing the photo-event (T).

In this paper, we propose also an original learning method to correct the estimation of the depth of interaction. We report experimental results corroborating the temporal imaging technique, by showing the benefit of using the temporal data provided by the Digital Philips Photon Counter device in order to better localize the photoelectric event in space, time and energy.

2. OBSERVED PARAMETERS WITH EXISTING ELECTRONICS

By using today's electronics, it is not possible yet to make a snapshot of the first photons detected 1 ns after each interaction. Using Philips DPC,[4] we have found that it is possible to observe for a group of 4 pixels denoted a die, the time of arrival of the first photon. Besides, for each pixel, it is possible with Philips DPC to count the number of photons detected during a scintillation event. The DPC-3200-22 sensor consists of 16 independent die sensors arranged in a 4×4 array. Thus, we have the photon distribution with a granularity of 4×4 mm and the time distribution with a granularity of 8×8 mm. A die sensor contains four pixels, arranged in a 2×2 array, and each pixel consists of 3200 SPAD cells. A pair of time to digital converters (TDCs) is coupled to each die and generates a single timestamp. The timestamp generation is determined by the configured trigger threshold, which can be set to the level of the first photon or, alternatively, to higher photon thresholds. We choose to use first photon trigger level during our measurements, in order to get the best timing performances.

Experimental acquisition set-up: We used a LYSO crystal $32 \times 32 \times 20$ mm with a polished exit face coupled with optical grease to the Philips DPC Tile. All the other faces are roughened and covered with Teflon to ensure a diffusive return of the photons non directly detected and a collection of as much as possible photons to have a good estimation of the energy of each event. The crystal is 20 mm distant from a 0,5 MBq 22Na source. The crystal and the tile are enclosed in a dedicated mechanical housing to prevent stray light. The experiment is carried inside a controlled temperature chamber to prevent temperature variation during the acquisition.

Calibration in energy and quantum efficiency of the system: We have acquired 1000s of data in order to calibrate the set-up in energy. Our objective here is to calibrate our set-up against the 511 KeV 22Na peak. Hence, our data processing rejects low energy events. As Philips DPC counts detected photons, it is quite straightforward to estimate the average quantum efficiency of the system as a whole. Assuming an LYSO light yield of 25000 ph/Mev, we find an average quantum efficiency, filling factor included, of 27% for the complete tile, quite in line with Philips Data. We then assume that the relationship between the number of detected photons and Energy is linear in the range 400-1000 KeV. We observed an energy resolution of 10,8% @ 511 KeV and a position of the photo-peak @ 2600 counts.

3. EXPLOITING LIGHT AND TIMING DISTRIBUTION OF A PHOTOELECTRIC EVENT

Figure 1 illustrates the principle of temporal imaging. The first detected photons are the un-scattered ones filling a disc whose radius is related to the depth of interaction. The scattered photons will be detected later according to a random scattering process on the crystal faces, randomly filling the whole detector plane. The temporal information could then be used in order to a have a clean image of the photo-electric event.

3.1 Energy localization

Once an event is validated at the die level, the Philips system records the time when the first photon is detected and the energy deposited on each pixel of the die during the integration time (620 ns). We correct this data log for time skew and organize it according to the corrected time in a matrix, discarding low energy events. This gives an event matrix yielding:

- The number of photons detected by each pixel during the integration time. This value is written on the image shown in Figure 2 below with also a color code.
- The time stamp when the first photon is detected on each die. The first photon detected for each event is taken as 0. We thus keep only the difference (in units of 19,5 ps) between other dies and this initial die. All our analysis is based on this time difference. This value is written at the intersection of the 4 pixels composing a die (Figure 2).

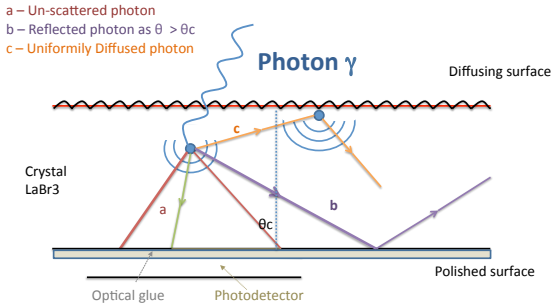

Figure 1: Illustration of emitted photons behaviors before detection on the Si-PM

For each event, we have then a joint visualisation of the light distribution and the time distribution. For instance, observing the event reported in Figure 2, one can validate a photo-electric event as its light distribution is symmetric with respect to the estimated barycentre. If a single Compton event was present, the light distribution would be axisymmetric. Through time gating, the spread of the light distribution could also be reduced. In fact, an important parameter in temporal imaging is the characteristic transfer time, defined as the time taken by an UV photon to cross the thickness of the scintillator. In our case, TT is approximately equal to 122 ps. Diffused photons have typically a much longer path, most of them bounce back on the top before coming back. Hence they arrive later than twice the transit time (244ps = 12 timestamp units in our experimental set-up). For this event of Figure 2, the total number of detected photons is 3498 vs 2600 event for 511 KeV photo-peak. Hence the energy is 715 KeV.

3.2 Spatio-Temporal localization

A first advantage of exploiting the time information is to compute the barycentre (X, Y) and the depth of interaction (DOI) at a well-defined time after the first detected photon. Estimating the localization too early may suffer from the low number of detected photons with less robust statistics. On the other hand, estimating the localization too late may be perturbed by photons detected later after being scattered on the crystal faces.[1] A careful decision time is then crucial for the detection performances. While increasing the decision timing, it was observed that the localization error decreases until reaching its minimum and then it increases in a monotone way. Consequently, a practical choice of the decision time could be between 500 ps and 750 ps as the number of detected photons is at least 100, which ensures the robustness of the statistical estimation of the critical disc.

Concerning the estimation of the depth of interaction (Z), we propose, in this paper, an original method based on the estimation of a function mapping the local light distribution to the depth of interaction Z. This consists in extracting a local descriptor (both in space and time) based on the proportion of an 8-neighborhood pixel intensities with respect to the total plane detected intensity. Time gating allows filtering noisy and irrelevant data. The mapping function is computed by learning a polynomial relation based on simulated learning data. To illustrate the difference between the proposed method (temporal filtering) and the classical estimation technique (without using temporal information), figure 3 reports the localization estimation of both techniques on the same photo-electric event. It can be noted that the classical method (Figure 3-(a)) suffers from the photons scattered on the crystal faces and detected later. However, the use of the temporal information allows an accurate estimation of the barycentre and also an accurate estimation of the depth of interaction (Figure 3-(b)). In order to better (experimentally) illustrate the performances of the proposed temporal technique, Figure 4 shows the cloud of computed barycentres with a continuous 0,5 MBq 22Na source, with a classical method (Figure 4-(a)) and with time-corrected method (Figure 4-(b)). The spatial distribution of the interaction barycentres corroborates the relevance of the use of the temporal information. With the proposed method, the barycentres are equally distributed on the whole plane, which is in line with their actual distribution. However, with the classical method, the estimated spatial distribution is distorted with respect to the actual one.

4. CONCLUSION

In this work, he have proposed an original time-based imaging concept for accurate spatio-temporal localization of scintillation events within a monolithic scintillator and a digital Si-PM matrix. Combining the light distribution and first detected photons arrival time distribution, it was possible to extract an efficient descriptor in order to identify a photoelectric event and to accurately localize it in space, time and energy. Experimental results corroborate the temporal imaging technique, using the temporal data provided by the Digital Philips Photon Counter device. Achieved Gamma interaction online localization precision (around 1x1x2 mm) in monolithic scintillators is very promising for accurate and online PET imaging. The availability of very fast mixed ASICs[7] is also promising for enhancing the performance of temporal imaging.

ACKNOWLEDGMENTS

This work is supported by ANDRA under the PIA TEMPORAL project.

REFERENCES

1. Alain Iltis and Hichem Snoussi , The Temporal PET Camera: A New Concept With High Spatial and Timing Resolution for PET Imaging,J. Imaging 2015, 1(1), 45-59; doi:10.3390/jimaging1010045
2. Iltis, A., Mayhugh, M. R., Menge, P., Rozsa, C. M., Selles, O., and Solovyev. Lanthanum halide scintillators: Properties and applications. Nuclear Instruments and Methods in Physics Research Section A: Accelerators, Spectrometers, Detectors and Associated Equipment, 563(2), 359-363, 2006
3. Stefan Seifert, Herman T van Dam, Jan Huizenga, Ruud Vinke, Peter Dendooven, Herbert Lohner and Dennis R Schaart , Monolithic LaBr3:Ce crystals on silicon photomultiplier arrays for time-of-flight positron emission tomography, Phys. Med. Biol 57 (2012) 2219-2233.
4. Thomas Frach, Gordian Prescher, Carsten Degenhardt, Rik de Gruyter, Anja Schmitz, and Rob Ballizany , The Digital Silicon Photomultiplier Principle of Operation and Intrinsic Detector Performance, 2009 IEEE Nuclear Science Symposium Conference Record (NSS/MIC)
5. 1 Anger, H. O, Gamma-ray and positron scintillation camera. Nucleonics (US) Ceased publication, 21(UCRL-10933), 1963
6. Pani, R., Vittorini, F., Pellegrini, R., Bennati, P., Cinti, M. N., Mattioli, M., and De Notaristefani, F. (2008, October). High spatial and energy resolution gamma imaging based on LaBr3 (Ce) continuous crystals. In Nuclear Science Symposium Conference Record, 2008. NSS'08. IEEE (pp. 1763-1771).
7. J Fleury, S Callier, C de La Taille, N Seguin, D Thienpont, F Dulucq, S Ahmad and G Martin, Petiroc and Citiroc: front-end ASICs for SiPM read-out and ToF applications 2014, JINST 9 C01049

8. Lewellen TK, Murano R. A comparison of count rate parameters in gamma cameras.J Nucl Med. 1981 Feb;22(2):161-8.
9. Adam LE1, Karp JS, Daube-Witherspoon ME, Smith RJ.Performance of a whole-body PET scanner using curve-plate NaI(Tl) detectors.J Nucl Med. 2001 Dec;42(12):1821-30.
10. Alain Iltis, Systeme et Procede de detection de rayonnement gamma de type gamma camera. Patent FR 1260596. Nov 2012.
11. Seiichi Yamamoto. Development of Si-PM Based Imaging Systems for Molecular Imaging. Journal of Medical and Bioengineering Vol. 2, No. 1, March 2013
12. Jarritt PH1, Acton PD. PET imaging using gamma camera systems: a review.Nucl Med Commun. 1996 Sep;17(9):758-66.

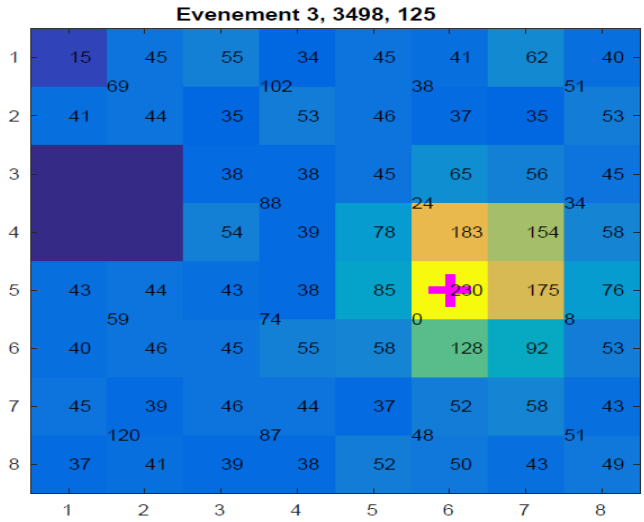

Figure 2: An instance of a photo-electric event detection: we report the number of detected photons per pixel and the first arrival time per die (a group of 4 pixels).

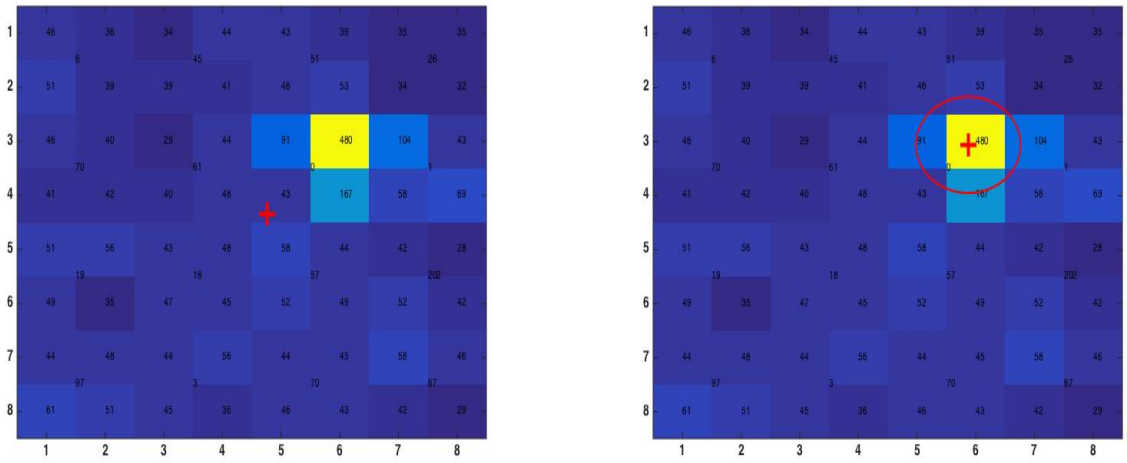

(a) (b)

Figure 3: An instance of a photo-electric event detection. (a) 2D localization (red cross) with a classical method, (b) 2D (red cross) and DOI (red circle) localization with the proposed method.

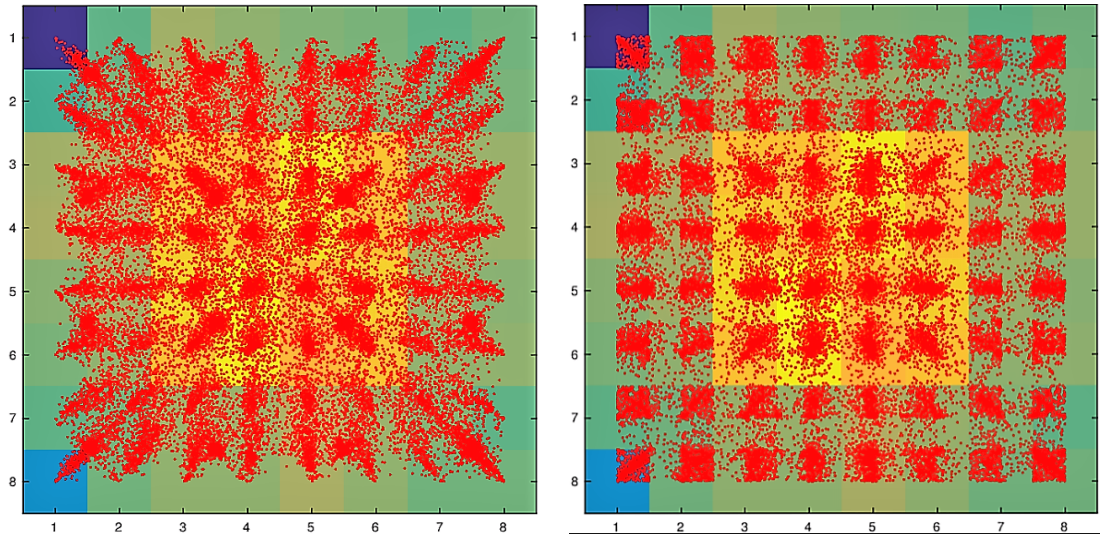

(a) (b)

Figure 4: (a) Could of computed barycentres for a continuous 22Na source with a classical method, (b) Could of computed barycentres for a continuous 22Na source with the proposed method.